Radioprotective effects of valproic acid, a histone deacetylase inhibitor, in the rat brain

YONG ZHOU*, JUNJIE NIU*, SHUPENG LI, HUAYING HOU, YING XU, WEI ZHANG and YUHUA JIANG

Cancer Centre, The Second Hospital of Shandong University, Jinan, Shandong 250033, P.R. China

Received July 16, 2014; Accepted August 27, 2014

DOI: 10.3892/br.2014.367

Abstract. Radiotherapy is commonly used in the treatment of brain tumors but can cause significant damage to surrounding normal brain. The radioprotective effects of valproic acid (VPA) on normal tissue in the rat brain were evaluated following irradiation. Male Wistar rats were used in the present study and 48 rats were randomly divided into four groups consisting of 12 rats each. The whole-brain irradiation (WBI) was delivered by X-ray and the rats received the following treatment once a day for 5 days. The control group (sham-exposed group) received sham irradiation plus physiological saline. The VPA group received sham irradiation plus 150 mg VPA/kg. The X-ray group received WBI plus physiological saline. The combined group received WBI plus 150 mg/kg intraperitoneally VPA. A total of 6 months post-irradiation, the rats were sacrificed and the brains were harvested. Cell apoptosis in the cortex was determined by immunohistochemistry 24 h post-irradiation using an antibody for protein caspase-3. Transmission electron microscope (TEM) analyses were used to assess the effects of VPA on the radioprotection of rat normal brain cells 6 months post-irradiation. The weights of the animals in the TEM group measured over the two weeks after the first injection of VPA were also observed. Histological findings demonstrated that apoptosis occurred on the cortex 1 day after treatment, peaking in the X-ray group. The cells of the combined group showed a moderate caspase-3 staining compared to the X-ray group. There was a trend towards a lower body weight of the X-ray group following irradiation compared to either no-irradiation or rats of the combined group, although there was no significant difference in the average weight between the combined group and irradiated rats. Mild swelling of the capillary endothelial cells in the irregular lumen was observed in the combined group, whereas the X-ray group showed a severe structural disorder. In conclusion, VPA supplementation during radiotherapy may be beneficial for radioprotection following WBI by reducing normal brain cell injury.

Correspondence to: Professor Yuhua Jiang, Cancer Centre, The Second Hospital of Shandong University, 247 Beiyuan Street, Jinan, Shandong 250033, P.R. China
E-mail: jiangyuhua@sdu.edu.cn

*Contributed equally

Key words: fractionated radiotherapy, valproic acid, brain injury, radioprotection

Introduction

Radiotherapy has an increasingly notable role in the treatment of the majority of malignant and a number of benign neurological neoplasms, and the treatment of select nonmalignant entities (1). However, the maximum radiation dose that can be used is limited by the tolerance of normal tissues surrounding the tumor (2). Thus far, in order to reduce radiotherapy-induced central nervous system (CNS) damage, several attempts are being made. One of these approaches is to apply the total dose locally in fractions, in order to preserve healthy neural tissue. Additionally, searches for novel treatment opportunities to prevent radiation damage are continuing. Following this, newer therapeutic methods may help diminish the risks of radiotherapy by not limiting the volume treated.

Histone deacetylase (HDAC) inhibitors represent a novel class of radiation protectors and mitigators against total-body irradiation and can produce a significant reduction in injury even when administered following the radiation exposure (3). Various mechanisms have been proposed for the radioprotective effects of HDAC inhibitors (4-6). Valproic acid (VPA) (Fig. 1), a HDAC inhibitor, is frequently prescribed as an anti-epileptic drug in patients with brain tumor due to its effectiveness, oral bioavailability and generally low toxicity profile (7-10). Previous findings have shown that VPA enhanced the radiation response of various brain tumor cell types *in vitro* and *in vivo* (11-14). Notably, VPA not only radiosensitizes tumor cells, but it may also protect normal brain from radiation.

Results from the study by Lai *et al* (15) indicate that VPA may decrease human neural cells vulnerability to cellular injury evoked by oxidative stress, possibly arising from putative mitochondrial disturbances involved in bipolar disorder. Similarly, VPA has neuroprotective effects in cultured cortical neurons undergoing spontaneous cell death. A previous study also indicated that the neuroprotective properties of VPA involve modulation of neurotrophic factors and receptors for melatonin, which is also believed to play a role in neuroprotection (16). However, it is also thought that VPA reduces DNA double-strand break repair capacity and increases radiosensitivity in fibroblasts obtained from healthy skin tissue (6).

The histological effects of radiation on normal brain tissues have been studied by numerous investigators and the morphological character described has generally been the same, regardless of species or the type of radiation used to induce the damage (17-20). The majority of these studies used single X-ray (17-19) rather than fractionated radiotherapy (FRT) (20,21) although fractionated radiation is more commonly used clinically. However, radioprotection of VPA in rat brain following moderate-dose FRT is not clearly understood.

To maximize the therapeutic ratio of a radiosensitizing agent, it is important that the drug does not enhance the radiation-induced toxicity of normal cells or tissue. The present study examined the whole-brain radioprotection of VPA following FRT *in vivo*. Tissue samples from Wistar rats treated with X-ray plus VPA were studied to gain a certain insight as to how the compound modifies the radiation response of normal brain. The primary goal was to perform evaluations of the cortex cell response following VPA and fractionated X-ray irradiation. The occurrence of radiation-induced apoptosis in normal brain was investigated using immunohistochemistry (IHC). The development of vascular changes in the rat brain was investigated by means of transmission electron microscope (TEM). Animal weights of the TEM group over 14 days starting from the injection of VPA were also observed.

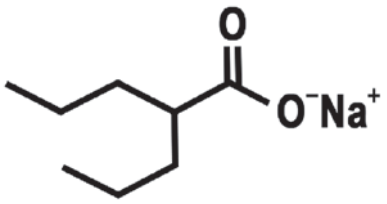

Figure 1. Structure of valproic acid.

Materials and methods

Animals. At the beginning of the experiment, male Wistar rats (Center for New Drugs Evaluation of Shandong University, Jinan, China), 8 weeks old and weighing ~180-190 g, were allowed to acclimatize for 1 week prior to the start of the study. The rats were maintained in environment-controlled (temperature and lighting) animal facilities, provided food and water *ad libitum* and randomly assigned to the experimental groups. All the studies were performed with prior approval and in accordance with Institutional and National standards of Animal Care.

Irradiation. The whole-brain irradiation (WBI) was delivered by X-ray (6 MeV-energy and 3 Gy/min). The rats were irradiated using a 6-MV linear accelerator (Elekta Synergy, Ltd., Stockholm, Sweden), under mild anaesthesia by chloral hydrate [30 mg/kg, intraperitoneally (i.p.)]. A total of four rats were placed in a reproducible way; in a prone position on the linac couch with laser alignment. The radiation field was 15x15 cm at a source-axis distance of 100 cm. The isocenter was in the midline of the brain and the posterior limit of the field corresponded to the line passing by the posterior section of the two ears (22). The dose was delivered according to the reading of the 'Ionex' ionization chamber, which was positioned directly above the skull. Dosimetry was performed by ion chamber and chemical Fricke dosimetry.

Experimental design. After 7 days of handling, 48 rats were randomly divided into four groups, consisting of 12 rats each. The control group (sham-exposed group) received sham irradiation plus physiological saline. The VPA group received sham irradiation plus 150 mg/kg VPA (sodium salt; Sigma, St. Louis, MO, USA). The X-ray group received X-ray WBI plus physiological saline. The combined group received X-ray WBI plus 150 mg/kg VPA. The dose of VPA used in the present study (150 mg/kg) was based on a previous study (11). The rats were administered 10 injections (150 mg/kg) over 5 days, by i.p. every 12 h. Following the third injection, FRT was delivered to the whole brain of the rats at a daily dose of 3 Gy, 5 days/week for 1 week, for a total of 15 Gy. Each group was randomly divided into two sections; one section was obtained for histological study using histology evaluation and the other was used for ultra-structural analysis under the electron microscope (EM). The animal weights of the TEM group over 14 days starting from the first injection of VPA were also observed.

IHC. IHC staining was used to confirm the presence of normal brain tissue damage in Wistar rats. One section of the rats was sacrificed and the brains were harvested. Animals were sacrificed 1 day after radiation using 0.4 mg/kg of chloral hydrate (i.p.) and were subsequently perfused with 100 ml (10 min) of saline before 500 ml (30 min) of 4% paraformaldehyde (Sigma) in phosphate-buffered saline (PBS) for histological analysis. The whole brain was collected and fixed in 4% paraformaldehyde at 4˚C overnight. The fixed brains were sliced coronally and embedded in paraffin wax. Radiation brain injury blocks were processed and cut into serial 4-μm sections for histology.

Cell apoptosis was analyzed in the cortex according to the method of IHC using protein caspase-3 (Sigma). Caspase-3 immunostaining was performed on sections from each group. The sections were washed in PBS and Tris-buffered saline and incubated with 10% normal goat serum for 30 min. The sections were incubated with a mixture of two monoclonal rat anti-mouse caspase-3 antibodies at a dilution of 20 mg/ml overnight at 4˚C. Following this, the sections were counterstained with hematoxylin (Sigma) and mounted with aqueous mounting media. All the measurements were performed in triplicate.

Histological images in the cerebral cortex overlying the dentate gyrus of the hippocampus (20) were acquired by digital photomicrography, using a light microscope under magnification, x10-200. The tissue sections were coded. Histopathological evaluation was carried out by two blinded pathologists at the Second Hospital of Shandong University.

TEM. TEM analysis was used to assess the effects of VPA on the radioprotection of rat brain microvascular. At an interval of 6 months after irradiation, groups of rats were sacrificed under deep chloral hydrate anaesthesia (400 mg/kg) for the other sections. The brains were removed quickly and the regions of interest on the cortex (overlying the dentate gyrus of the hippocampus) (20) were removed quickly and sliced into 1.0-mm

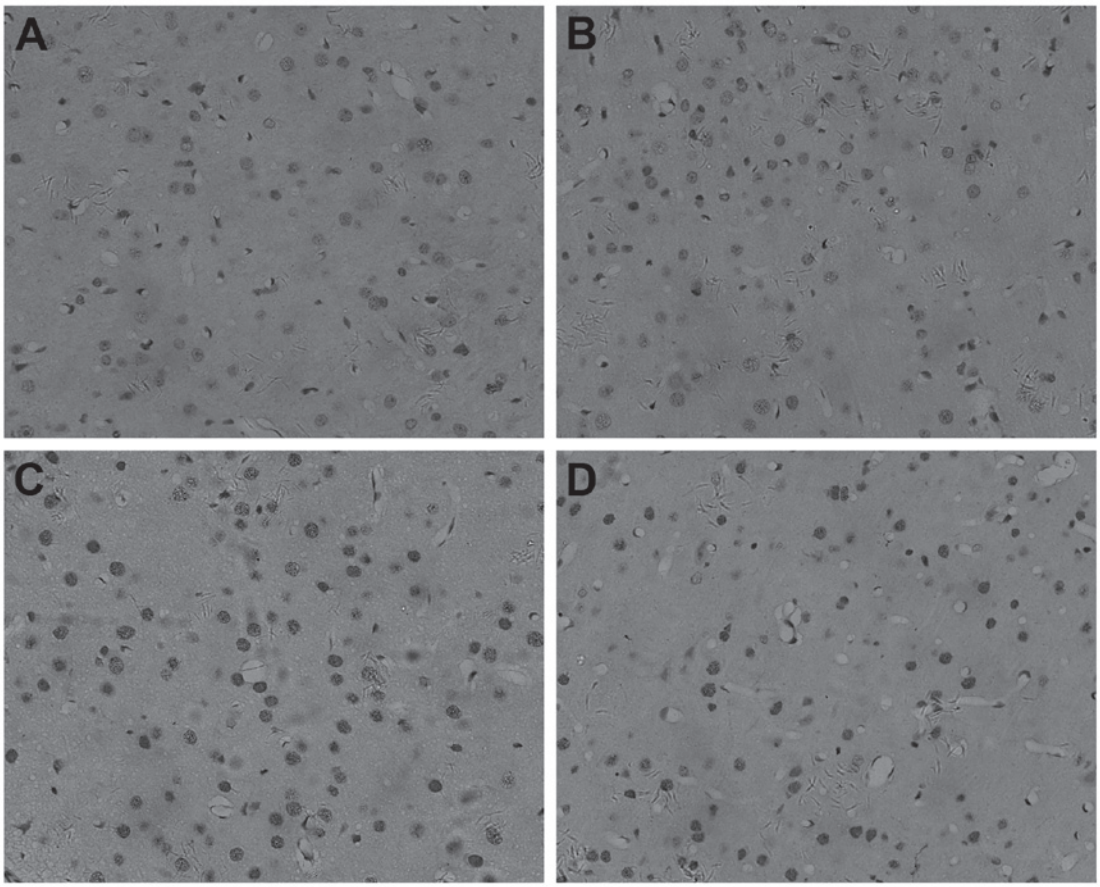

Figure 2. Apoptosis analysis of cerebral cortex at 24 h (magnification, x200). The (A) control, (B) valproic acid, (C) X-ray and (D) combined groups. Cell apoptosis was analyzed in the cerebral cortex according to the method of immunohistochemistry using protein caspase-3. All micrographs are magnification, x200.

sections prior to fixing in cold EM grade 2.5% glutaraldehyde in 0.1 mol/l PBS (pH 7.3). Subsequently, the sections were rinsed in PBS, postfixed in 1% OsO_4 with 0.1% $K_3Fe(CN)_6$, dehydrated through a graded series of EtOH and embedded in Epon (dodecenyl succinic anhydride, nadic methyl anthydride, Scipoxy 812 Resin and dimethylaminomethyl; Energy Beam Sciences, East Granby, CT, USA). Ultrathin sections (65-nm) were cut and stained with 2% uranyl acetate and Reynold's lead citrate, and examined on a JEM-1011 TEM (Jeol, Tokyo, Japan). The sections were qualitatively analyzed for the degree of radiation injury by blinded investigators, unaware of the experimental condition.

Statistical analysis. For statistical analyses, Statistical Product and Service Solutions software package (SPSS, Inc., Chicago, IL, USA) was used. The statistical significance of the experimental data among the groups was assessed with the Student's t-test. All the values were expressed as mean ± standard deviation for $n \geq 3$. $P<0.05$ in each experiment was considered to indicate a statistically significant difference and statistical power was calculated accordingly.

Results

IHC slide of the rat brain at the 15 Gy dose level. Cell apoptosis was quantified using a protein caspase-3 and a morphological assessment of cell staining (original magnification, x200). These sections were from the cerebral cortex overlying the dentate gyrus of the hippocampus. Oligodendrocytes and their processes stain dark brown (Fig. 2). By IHC, caspase-3 was found to be present mainly in the nucleus of cells in the unirradiated cortex of oligodendrocyte (Fig. 2A and B). Following irradiation, the number of positive nuclei and the intensity of the reaction product were greatly increased (Fig. 2C and D).

Apoptosis occurred in the cortex 1 day after treatment, peaking in the X-ray group (Fig. 2C). The cells of the combined group (Fig. 2D) showed moderate caspase-3 staining in the cytoplasm and nucleus. Caspase-3 was significantly decreased in the combined group (Fig. 2D) compared to the X-ray group (Fig. 2C) in the cortex of the brain. Caspase-3 had the lowest expression in the control (Fig. 2A) and VPA groups (Fig. 2B).

Animal weight throughout the course of the experiment. Following the third injection of VPA, 15 Gy (3 Gy/day) was delivered locally to the brain over five days. The FRT treatments were well tolerated by all the animals, as no apparent adverse effects were observed in any group throughout the course of the study. The animal weights of the TEM group over two weeks starting from the injection of VPA were also observed. Following VPA and irradiation, there were significant differences in the average weight of the animals between the combined and control groups, on day 6, 12 and 14 day ($P<0.05$) (Table I). By contrast, two days after irradiation the average weight of the X-ray group was significantly less

Table I. Animal weights of the TEM group over 14 days starting from the first injection of valproic acid (VPA).

	Day							
Group	0	2	4	6	8	10	12	14
Combined[a]	236.00±5.329	248.33±9.832	248.00±13.115	249.50±14.653[b]	252.50±16.991	259.50±16.742	267.50±18.097[b]	278.17±25.795[b]
X-ray[a]	233.67±17.072	242.33±25.586	241.83±29.404[b]	236.83±37.156[b]	236.50±40.134[b]	243.17±42.466[b]	257.00±42.506[b]	272.50±41.215[b]
VPA[a]	231.83±7.250	245.67±9.647	250.33±10.930	266.17±13.258	270.67±11.308	273.83±12.007	297.83±11.125	320.83±13.834
Control[a]	237.33±7.866	259.00±13.446	268.33±14.109	279.17±15.342	280.17±15.715	287.33±14.404	298.67±13.909	316.67±16.182

[a]Data are presented as average weight (g) ± standard error of the mean. [b]P<0.05 vs. untreated control group. Total number of animals, n=24. TEM, transmission electron microscope.

than that of the controls (P<0.05) (Table I). There was a trend towards a lower body weight in X-ray group following irradiation compared to either no-irradiation or rats of the combined group (Fig. 3), although there was no significant difference in the average weight between the combined group and irradiated rats (Table I). However, two days after VPA, the weight change of the average weight in the combined group was characterized by a plateau from days 2-8 and a steep increase following irradiation, compared to the X-ray group (Fig. 3B). A tendency of an increase for the average body weight of combined group at 15 Gy was evident, but this difference was not statistically significant (Fig. 3B)

Observation of ultrastructure. TEM analysis was also used to assess the radioprotection of VPA on the cortex cells of rat normal brain. The development of vascular changes in the rat brain following a moderate-dose FRT X-ray (15 Gy) was investigated. The results indicate that, even with this dose, vascular abnormalities occur 6 months after irradiation. The X-ray group (Fig. 4C) showed a severe structural disorder, loss and thickening of microvascular wall, hyaline degeneration and fibrosis generally changed. Focal swelling of the capillary endothelial cells can be detected with the TEM method in the combined group (Fig. 4D). Mild swelling of the capillary endothelial cells in the irregular lumen was observed. However, the control (Fig. 4A) and VPA groups (Fig. 4B) exhibited normal vessel walls with well-preserved tight junctions.

Discussion

In the present study, the dose to the brain was purposely limited to 15 Gy. This dose level was selected on the basis that the induced effects should be similar to the ones observed in the human brain following a full course of FRT. Moderate-dose fractionated X-ray irradiation did not appear to affect the rat well-being. Whereas there is no doubt that a higher dose will result in the earlier appearance of gross damage, the underlying pathology may be quite different. This schedule was designed to allow us to assess the acute and late effects of brain irradiation. As there was no precedence to follow, 1 day and 6 months were chosen as an adequate interval to investigate the changes induced by FRT. The experiments were terminated at 6 months after the start of FRT, which were considered to be sufficient to observe the late changes induced by radiation treatment.

Previous studies have reported that exposure to HDAC inhibitors does not increase the radiosensitivity of various normal tissue cell lines (12,23,24), whereas certain HDAC inhibitors inhibit the repair of radiation-induced DNA double-strand break and increase radiosensitivity of normal cells, specifically lymphocytes (25) and primary skin fibroblasts *in vitro* (6). Additionally, *in vitro* and *in vivo* data indicate that HDAC inhibitors may protect normal tissue from radiation-induced side effects (4,26).

Irradiation has been shown to induce apoptosis in oligodendrocytes *in vivo* (27-30) and *in vitro* (31). Stress-induced oligodendrocyte apoptosis was mediated by caspase activation (32). Caspases are cysteine proteases that play a key role in cascade activation during apoptosis induced by a number of stimuli (33-36). In addition to cell death, the active caspase-3 plays a role in normal cellular processes, including neuronal differentiation and migration. The results of the study by Soane *et al* (37) indicate that upregulation of B-cell lymphoma 2 protein and inhibition of caspase-3 activation are potential mechanisms by which C5b-9 increases survival of oligodendrocyte *in vitro* and possibly *in vivo* during inflammation and immune-mediated demyelination affecting the CNS. Although caspases, including caspase-3, are activated following ionizing radiation, it has also been indicated that the radiation-induced apoptosis is not dependent on them in the developing CNS (38). However, using primary cultures of neural precursor cells of the cortex from developing rat brain, the study by Michelin *et al* (39) demonstrated the protection from radiation-induced apoptosis by caspase-3 inhibitor is involved in the apoptotic mechanism.

To investigate the signaling pathways implicated in the radioprotection-induced apoptosis of the rat cortex cells in the four groups, an IHC analysis was used to examine the caspase-3 protein levels. Subsequently, the present study demonstrated that irradiation induces an evident increase of caspase-3 activity in oligodendrocytes irradiated *in vivo*. In addition, caspase-3 was significantly decreased in the combined (Fig. 2D) compared to the X-ray group (Fig. 2C) on the cortex of the brain. The results of the study demonstrated that exposure to VPA leads to a decrease in radiation-induce apoptosis in the rat cortex. Caspase-3 had the lowest expression in the control (Fig. 2A) and VPA groups (Fig. 2B). These results indicate an important role of VPA in irradiation-induced apoptosis. As a result, although quantitative studies to determine the proportions of the different cellular types affected

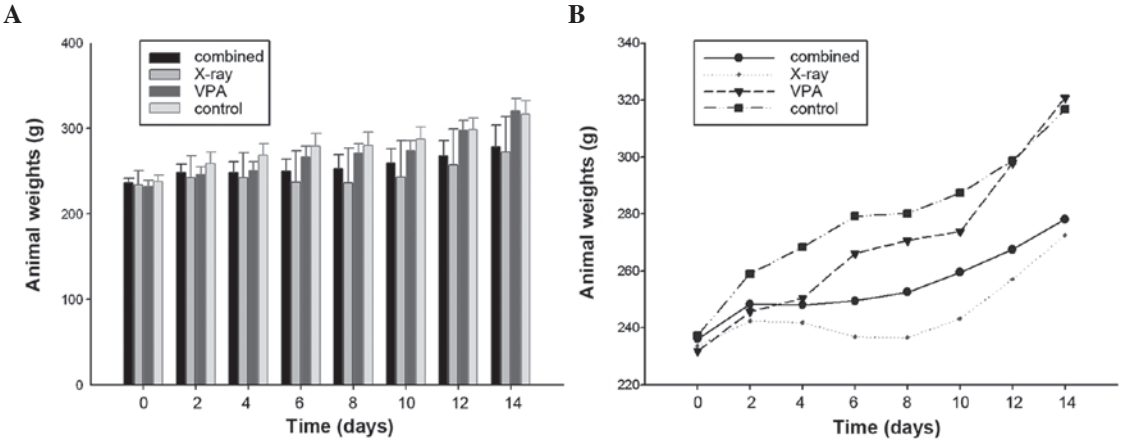

Figure 3. Animal weight over 14 days. P<0.05 vs. untreated control group. Animal weights of TEM group over 14 days starting from the first injection of valproic acid (VPA) were observed. Each bar represents the mean value of 6 animal weights and error bars are standard error of the mean. Total number of animals, n=24.

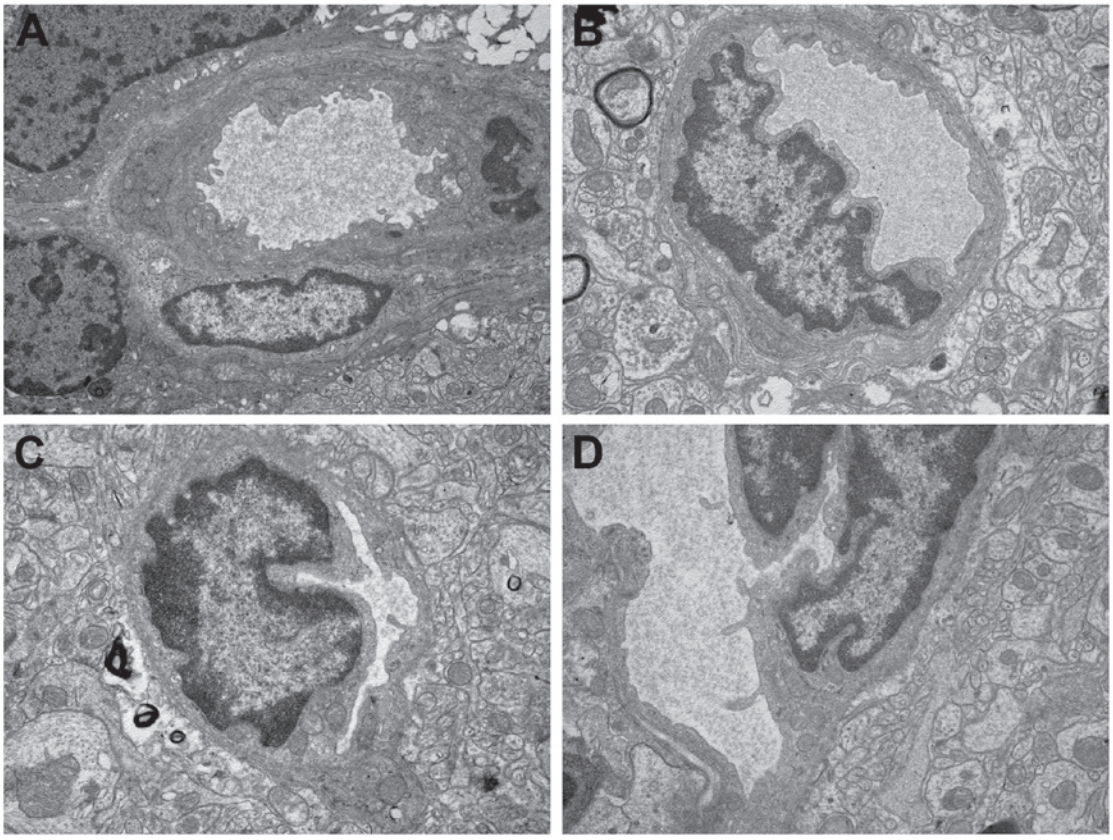

Figure 4. Vascular changes of brain tissue 6 months after irradiation (magnification, x15,000). Ultrastructural features of valproic acid-induced radioprotection in normal brain cells. The (A) control, (B) valproic acid, (C) X-ray and (D) combined groups.

by X-irradiation and VPA injection were not carried out, the present data indicate that VPA, a HDAC inhibitor, developed a radioprotective effect from radiation-induced apoptosis of in the rat cortex.

Oligodendrocytes have been shown to undergo radiation-induced apoptosis in the CNS *in vivo*. An understanding of the signalling pathways in mediating radiation-induced apoptosis of oligodendrocytes may lead to targeting strategies that protect the CNS from radiation injury (30). Following radiation, cells undergo rapid sphingomyelin hydrolysis and ceramide generation followed by apoptosis (40). Results of the study by Ferrer (41) suggest that X-irradiation enhances naturally occurring cell death in the cerebral cortex and subcortical white matter and that this process depends on the activation of protein synthesis. On the basis of previous studies regarding cell death (Fig. 4) *in vivo*, one could expect that oligodendrocytes death caused by X-ray would be inhibited after an i.p. injection of VPA. Furthermore, the detection of caspase-3 induction in the cortex, indicates that the cortex has an acute response to radiation. Whether the expression of this stress protein contributes or protects against the generation of the late radiation injury remains to be determined. The cardinal

features of radiation exposure of the CNS are demyelination, gliosis and vascular damage (42).

Following irradiation with a single dose of 8, 18 or 22 Gy, a peak response was observed at ~8 h after irradiation in the rat spinal cord, and the apoptosis index returned to the levels in non-irradiated oligodendrocytes at 24 h (28,43,44). The present result (Fig. 2) showed the activation of caspase-3 in irradiated oligodendrocytes 24 h after IR. The fractionated irradiation dose of 15 Gy-induced apoptosis was mediated by caspase-3 in oligodendrocytes. Morphologically, apoptosis in 8-week-old rat cortex appeared to be confined to oligodendrocytes cells and little evidence of apoptosis was found in neurons and vascular endothelial cells. Vascular and glial changes are significant in the development of late radiation damage to the nervous system. Vascular effects occur at lower dose levels, but following a longer latent period with effects mediated through damage to neuroglia (45).

WBI of rats with 15 Gy X-ray has been reported to suppress cerebral glucose utilization in 1 month (46) and decreased cerebrovascular volume in ~1 year (47). Electron microscopic examinations in the study by Kubota *et al* (48) showed that injury in CNS has initiated within 1 week after the application of radiation. The present results indicated that even with the dose of 15 Gy FRT, the X-ray group showed a severe structural disorder in 6 months. To a certain extent, these findings are in accordance with a previous study in which cerebral endothelial cells are more sensitive to radiation damage than astrocytes (49). Mild swelling of capillary endothelial cells in the irregular lumen could be observed in the combined group. The findings indicate the protective effects of VPA pretreatment from radiation injury of the CNS partially at this dose. However, only a small local was observed in EM and further studies are required to improve the effect of VPA on the treatment of radiation injury. Subsequently, further study for ultrastructure changes of rat nerve caused by X-ray is required.

These data indicate a possible association, not necessarily causal, between the damage of the microvascular/oligodendrocytes unit of tissue injury and development of radiation-induced brain injury following the exposure of rats to conventional fractionation (21). The average weight of the irradiated animals was significantly lower than that of the sham-treated animals when assessed 30 days from the start of FRT, with a daily dose of 2 Gy delivered 5 days/week (total, 40 Gy) (20). In the present study, there was a trend towards the lowest body weight in the X-ray group following irradiation, when a 3 Gy daily dose was delivered 5 days/week (total, 15 Gy). Compared to the X-ray group, a tendency of an increase in body weight for the combined group was evident. However, this difference was not statistically significant ($P>0.05$). The observation time may be too short for assessment of body weight change.

Following WBI, there is a sequence of cellular events involving cell apoptosis and cerebrovascular change. Although it is unclear how experimental results obtained from animal models may be applied clinically, it is possible that such results can be used together with theoretical models of radioprotection. Animal models may also be used to test drug therapies that may ameliorate radiation injury to normal brain.

In conclusion, the present results demonstrate that VPA evidently provides radioprotection to the cortex of rats against the X-ray injury. Thus, treatment with VPA in combination with radiotherapy could be a noteworthy approach for protection of the normal brain. Considering the surge of interest in radioprotection, such results may be useful for improving future clinical strategies of VPA. Although it is promising as a protector of radiotherapy, further studies with VPA are warranted.

Acknowledgements

The present study was supported by the Shandong Provincial Natural Science Foundation, China (grant no. ZR2010HM080). We are grateful to the Central Research Laboratory (The Second Hospital of Shandong University) for their technical assistance and generous support.

References

1. Melian E: Radiation therapy in neurologic disease. Handb Clin Neurol 121: 1181-1198, 2014.
2. Wong CS and Van der Kogel AJ: Mechanisms of radiation injury to the central nervous system: implications for neuroprotection. Mol Interv 4: 273-284, 2004.
3. Brown SL, Kolozsvary A, Liu J, Ryu S and Kim JH: Histone deacetylase inhibitors protect against and mitigate the lethality of total-body irradiation in mice. Radiat Res 169: 474-478, 2008.
4. Chung YL, Lee MY and Pui NN: Epigenetic therapy using the histone deacetylase inhibitor for increasing therapeutic gain in oral cancer: prevention of radiation-induced oral mucositis and inhibition of chemical-induced oral carcinogenesis. Carcinogenesis 30: 1387-1397, 2009.
5. Wu X, Chen PS, Dallas S, *et al*: Histone deacetylase inhibitors up-regulate astrocyte GDNF and BDNF gene transcription and protect dopaminergic neurons. Int J Neuropsychopharmacol 11: 1123-1134, 2008.
6. Purrucker JC, Fricke A, Ong MF, Rube C, Rube CE and Mahlknecht U: HDAC inhibition radiosensitizes human normal tissue cells and reduces DNA double-strand break repair capacity. Oncol Rep 23: 263-269, 2010.
7. Peterson GM and Naunton M: Valproate: a simple chemical with so much to offer. J Clin Pharm Ther 30: 417-421, 2005.
8. Phiel CJ, Zhang F, Huang EY, Guenther MG, Lazar MA and Klein PS: Histone deacetylase is a direct target of valproic acid, a potent anticonvulsant, mood stabilizer, and teratogen. J Biol Chem 276: 36734-36741, 2001.
9. Göttlicher M, Minucci S, Zhu P, *et al*: Valproic acid defines a novel class of HDAC inhibitors inducing differentiation of transformed cells. EMBO J 20: 6969-6978, 2001.
10. Marks PA, Miller T and Richon VM: Histone deacetylases. Curr Opin Pharmacol 3: 344-351, 2003.
11. Camphausen K, Cerna D, Scott T, *et al*: Enhancement of in vitro and in vivo tumor cell radiosensitivity by valproic acid. Int J Cancer 114: 380-386, 2005.
12. Chinnaiyan P, Cerna D, Burgan WE, Beam K, Williams ES, Camphausen K and Tofilon PJ: Postradiation sensitization of the histone deacetylase inhibitor valproic acid. Clin Cancer Res 14: 5410-5415, 2008.
13. Van Nifterik KA, Van den Berg J, Slotman BJ, Lafleur MV, Sminia P and Stalpers LJ: Valproic acid sensitizes human glioma cells for temozolomide and γ-radiation. J Neurooncol 107: 61-67, 2012.
14. Zhou Y, Xu Y, Wang H, Niu J, Hou H and Jiang Y: Histone deacetylase inhibitor, valproic acid, radiosensitizes the C6 glioma cell line *in vitro*. Oncol Lett 7: 203-208, 2014.
15. Lai JS, Zhao C, Warsh JJ and Li PP: Cytoprotection by lithium and valproate varies between cell types and cellular stresses. Eur J Pharmacol 539: 18-26, 2006.
16. Castro LM, Gallant M and Niles LP: Novel targets for valproic acid: up-regulation of melatonin receptors and neurotrophic factors in C6 glioma cells. J Neurochem 95: 1227-1236, 2005.
17. Mizumatsu S, Monje ML, Morhardt DR, Rola R, Palmer TD and Fike JR: Extreme sensitivity of adult neurogenesis to low doses of X-irradiation. Cancer Res 63: 4021-4027, 2003.
18. Zabolotskii NN, Onishchenko LS and Galeev IS: Mitochondrial megaconia and pleioconia in the rat brain as possible adaptive reactions in conditions of lethal radiation and radiomodified lesions. Neurosci Behav Physiol 30: 497-501, 2000.

19. Yildirim O, Comoğlu S, Yardimci S, Akmansu M, Bozkurt G and Sürücü S: Preserving effect of melatonin on the levels of glutathione and malondialdehyde in rats exposed to irradiation. Gen Physiol Biophys 27: 32-37, 2008.
20. Yuan H, Gaber MW, Boyd K, Wilson CM, Kiani MF and Merchant TE: Effects of fractionated radiation on the brain vasculature in murine model: blood-brain barrier permeability, astrocyte proliferation, and ultrastructural changes. Int J Radiat Oncol Biol Phys 66: 860-866, 2006.
21. Cicciarello R, d'Avella D, Gagliardi ME, *et al*: Time-related ultrastructural changes in an experimental model of whole brain irradiation. Neurosurgery 38: 772-780, 1996.
22. Vinchon-Petit S, Janet D, Jadaud E, Feuvret L, Garcion E and Menei P: External irradiation models for intracranial 9L glioma studies. J Exp Clin Cancer Res 29: 142, 2010.
23. Munshi A, Kurland JF, Nishikawa T, *et al*: Histone deacetylase inhibitors radiosensitize human melanoma cells by suppressing DNA repair activity. Clin Cancer Res 11: 4912-4922, 2005.
24. Blattmann C, Oertel S, Ehemann V, *et al*: Enhancement of radiation response in osteosarcoma and rhabdomyosarcoma cell lines by histone deacetylase inhibition. Int J Radiat Oncol Biol Phys 78: 237-245, 2010.
25. Stoilov L, Darroudi F, Meschini R, van der Schans G, Mullenders LH and Nararajan AT: Inhibition of repair of X-ray-induced DNA double-strand breaks in human lymphocytes exposed to sodium butyrate. Int J Radiat Biol 76: 1485-1491, 2000.
26. Chung YL, Wang AJ and Yao LF: Antitumor histone deacetylase inhibitors suppress cutaneous radiation syndrome: Implications for increasing therapeutic gain in cancer radiotherapy. Mol Cancer Ther 3: 317-325, 2004.
27. Li YQ, Jay V and Wong CS: Oligodendrocytes in the adult rat spinal cord undergo radiation-induced apoptosis. Cancer Res 56: 5417-5422, 1996.
28. Chow BM, Li YQ and Wong CS: Radiation-induced apoptosis in the adult central nervous system is p53-dependent. Cell Death Differ 7: 712-720, 2000.
29. Atkinson SL, Li YQ and Wong CS: Apoptosis and proliferation of oligodendrocyte progenitor cells in the irradiated rodent spinal cord. Int J Radiat Oncol Biol Phys 62: 535-544, 2005.
30. Lu FG and Wong CS: Radiation-induced apoptosis of oligodendrocytes and its association with increased ceramide and down-regulated protein kinase B/Akt activity. Int J Radiat Biol 80: 39-51, 2004.
31. Vrdoljak E, Bill CA, Stephens LC, van der Kogel AJ, Ang KK and Tofilon PJ: Radiation-induce apoptosis of oligodendrocytes in vitro. Int J Radiat Biol 62: 475-480, 1992.
32. Gu C, Casaccia-Bonnefil P, Srinivasan A and Chao MV: Oligodendrocyte apoptosis mediated by caspase activation. J Neurosci 19: 3043-3049, 1999.
33. Lin HI, Lee YJ, Chen BF, *et al*: Involvement of Bcl-2 family, cytochrome c and caspase 3 in induction of apoptosis by beauvericin in human non-small cell lung cancer cells. Cancer Lett 230: 248-259, 2005.
34. Kim DS, Jeon SE, Jeong YM, Kim SY, Kwon SB and Park KC: Hydrogen peroxide is a mediator of indole-3-acetic acid/horseradish peroxidise-induced apoptosis. FEBS Lett 580: 1439-1446, 2006.
35. Zuliani T, Obriot H, Tual M, *et al*: Variable Bax antigenicity is linked to keratinocyte position within epidermal strata and UV-induced apoptosis. Exp Dermatol 17: 125-132, 2008.
36. Park SK, Kang H and Kwon CH: Caspase-dependent cell death mediates potent cytotoxicity of sulfide derivatives of 9-anilinoacridine. Anticancer Drugs 19: 381-389, 2008.
37. Soane L, Rus H, Niculescu F and Shin ML: Inhibition of oligodendrocyte apoptosis by sublytic C5b-9 is associated with enhanced synthesis of bcl-2 and mediated by inhibition of caspase-3 activation. J Immunol 163: 6132-6138, 1999.
38. Ferrer I: Role of caspases in ionizing radiation-induced apoptosis in the developing cerebellum. J Neurobiol 41: 549-558, 1999.
39. Michelin S, del Rosario Perez M, Dubner D and Gisone P: Increased activity and involvement of caspase-3 in radiation-induced apoptosis in neural cells precursors from developing rat brain. Neurotoxicology 25: 387-398, 2004.
40. Mathias S, Pena LA and Kolesnick RN: Signal transduction of stress via ceramide. Biochem J 335: 465-480, 1998.
41. Ferrer I: The effect of cycloheximide on natural and X-ray-induced cell death in the developing cerebral cortex. Brain Res 588: 351-357, 1992.
42. Brush J, Lipnick SL, Phillips T, Sitko J, McDonald JT and McBride WH: Molecular mechanisms of late normal tissue injury. Semin Radiat Oncol 17: 121-130, 2007.
43. Li YQ, Guo YP, Jay V, Stewart PA and Wong CS: Time course of radiation-induced apoptosis in the adult rat spinal cord. Radiother Oncol 39: 35-42, 1996.
44. Li YQ and Wong CS: Radiation-induced apoptosis in the neonatal and adult rat spinal cord. Radiat Res 154: 268-276, 2000.
45. Hopewell JW: Late radiation damage to the central nervous system: a radiobiological interpretation. Neuropathol Appl Neurobiol 5: 329-343, 1979.
46. Ito M, Patronas NJ, Di Chiro G, Mansi L and Kennedy C: Effect of moderate level X-radiation to brain on cerebral glucose utilization. J Comput Assist Tomogr 10: 584-588, 1986.
47. Keyeux A: Late modifications of cephalic circulation in head x-irradiated rats. Radiat Environ Biophys 13: 125-135, 1976.
48. Kubota Y, Takahashi S, Sun XZ, Sato H, Aizawa S and Yoshida K: Radiation-induced tissue abnormalities in fetal brain are related to apoptosis immediately after irradiation. Int J Radiat Biol 76: 649-659, 2000.
49. Fike JR, Gobbel GT, Chou D, Wijnhoven BP, Bellinzona M, Nakagawa M and Seilhan TM: Cellular proliferation and infiltration following interstitial irradiation of normal dog brain is altered by an inhibitor of polyamine synthesis. Int J Radiat Oncol Biol Phys 32: 1035-1045, 1995.